J Mater Sci (2007) 42:6477–6488
DOI 10.1007/s10853-007-1564-3

Impedance and modulus spectra of the percolation system silicon–polyester resin and their analysis using the two exponent phenomenological percolation equation

Godfrey Sauti · David S. McLachlan

Received: 16 October 2006 / Accepted: 29 January 2007 / Published online: 3 May 2007

Abstract The ac conductivity of silicon–polyester resin composites is found to be best fitted using the two exponent phenomenological percolation equation (TEPPE) (formerly known as the general effective media (GEM) equation). The results show that, with the actual experimentally measured components' electrical properties as input, the TEPPE can be used to model and fit the composites' complex conductivity data. The paper also highlights the importance of using several representations of the immittance spectroscopy data in order to correctly identify the various contributions, for instance the modulus plots clearly show the arcs due to the isolated percolation clusters, below the critical volume fraction.

Introduction

Composite materials have a wide range of technological applications, ranging from packaging to aerospace. Therefore, determining their properties and how these relate to those of the components and the microstructure is extremely useful. This enables us not only in understand and tailor the properties of existing materials but also to design new materials with a variety of applications.

G. Sauti · D. S. McLachlan
School of Physics and Materials Physics Research Institute, University of the Witwatersrand, P. Bag 3, Wits 2050, South Africa

G. Sauti (✉) · D. S. McLachlan
Department of Chemistry and Polymer Science, Stellenbosch University, P. Bag X1, Matieland 7602, South Africa
e-mail: godfrey_sauti@yahoo.com

The electrical properties of materials are of interest where it is intended to use these materials for electronic applications and in some cases, the desired properties are best obtained from composites. Further, electrical measurements can also be used as a tool for probing the properties of composites, including some whose intended applications are not necessarily electronic.

A number of silicon–polyester resin composites were prepared as described in the first part of the paper. The ac conductivity of these composites, which had varying volume fractions of silicon was then investigated. The investigation of the electrical properties was mainly carried out at 150 °C, where both the silicon and polyester resin conductivities were in a range where their properties could be resolved in impedance and/or modulus plots. At lower temperatures, the polyester resin was too highly insulating, while higher temperatures caused permanent changes in the polyester resin properties and ultimately led to the polyester resin's decomposition. Samples of the pure polyester resin were also prepared and their ac conductivity was measured, for use as fixed input when fitting the composite data. The electrical properties of the silicon, at 150 °C were obtained from fitting the composite data.

The experimental data is then fitted to the two exponent phenomenological equation (TEPPE). Simulations over a wide frequency and composition range are used explain all the qualitative features in the experimental data and the fitting.

Experimental

Sample preparation

A series of composites consisting of polyester resin and various volume fractions of high purity silicon powder

(99.998% silicon), obtained from Goodfellow Cambridge Limited, were prepared. The powder had an average particle size of 10 μm, measured, by the authors, using a Malvern particle size analyzer. The polyester resin (Tradename: Resin 1935) was obtained in the unpolymerized form. A catalyst (Tradename: Butanox M50), to speed up the polymerization process, was also obtained from the same source as the polyester resin. Resin 1935, the catalyst and between 0 and approximately 40 vol.% silicon were thoroughly mixed by stirring and the mixture was then left to set. The mixing was carried out until the onset of gelation of the polyester resin (approximately 10 min). This prevented the silicon from settling. The highly viscous resin/silicon mixture was stirred very slowly to minimize the formation of air bubbles. Disks, 10 mm thick and 22 mm in diameter, were cast in teflon molds. The upper limit to the amount of silicon that could be loaded into the polyester resin was that for which the polyester resin could still bind together to make a stable compact, without external pressure. The specimens were left in the molds for 36 h to ensure that the polymerization process had continued to completion, as per the supplier's instructions. The compacts obtained were able to fully retain their shape when removed from the molds. Specimens from the molds were then '' matured'' in a dry environment for 7 days, after which they were annealed, in air, at 160 °C for 12 h. The above procedure ensured that the samples' electrical properties were stable for the duration of the ac conductivity measurements at 150 °C. After annealing, the initial 10 mm thick disks were sliced into 3 mm thick specimens, for the measurements, using a diamond wafering blade. A list of the compositions of the silicon–polyester resin composites produced and the names used to refer to them is given in Table 1.

The distribution of the silicon in the silicon–polyester resin composites was analyzed using a Carl Zeiss Axiotech optical microscope. Specimens for optical microscopy, were polished with (100 and 200) grit silicon carbide paper and finished off with a polishing cloth and 1 μm alumina paste. This procedure gave a shiny polished surface.

Colloidal silver (Electrodag 1415, Acheson Industries) was applied onto the sample surfaces to form parallel plate capacitor specimens, for the electrical measurements. After the maturation and heat treatment, described above, the polyester resin was found not to readily dissolve in the solvent in which the colloidal silver was suspended (amylacetate). In spite of this, the solvent was evaporated rapidly, using a 60 W incandescent bulb as a heat source, to ensure that there was as little contact time as possible with the sample surface. After drying, the continuity of each electrode was tested by checking that the resistance between any two extreme points was less the 1 Ω on a Wavetek (DM28XT) resistance meter. Where electrodes did not meet this specification, they were polished off using 200 grit silicon carbide paper and reapplied. The samples, ready for measurement, were stored in a dry environment.

Impedance measurements

Ac conductivity measurements were carried out using a Novocontrol Broadband Dielectric Converter (BDC) in combination with a Solartron SI1260 Impedance/Gain-Phase Analyzer. The BDC + Solartron combination has an impedance measurement range of 10 Ω to 200 TΩ at frequencies ranging from 10 μHz to 10 MHz and a tan(δ) resolution < 0.1 mrad [1]. A sample excitation voltage of 1.5 V was used.

The investigation of the electrical properties was mainly carried out at 150 °C, where both the silicon and polyester resin conductivities were in a range where the contributions of the components could be resolved in the impedance and/or modulus plots. At lower temperatures, the polyester resin was very highly insulating, while higher temperatures caused permanent changes in the polyester resin properties and ultimately led to the polyester resin's decomposition. The sample temperature was monitored and controlled to ±0.1 °C by a LakeShore DRC93-CA controller. This controller received input from the PT100 platinum resistance thermometer mounted on the sample stage of a temperature controlled furnace [2]. Samples were maintained in a rotary pump vacuum of ~10 mTorr to minimize atmosphere induced variations in the properties.

To enable easy comparison of data from samples of different sizes, Z', Z'' and the term *impedance* will be used to describe the *specific impedance*, i.e., the impedance independent of the sample geometric factor. The *specific impedance* (Z^*, in Ω m) is related to the directly measured sample impedance (Z_s^*, in Ω) by $Z^* = GZ_s^*$. The sample geometric factor is G (= A/L), where A is the sample cross-sectional area and L is the sample thickness. Other representations of ac impedance data are used in this work and these are related to the specific impedance by:

$$\text{Modulus: } M^* = \mathrm{i}\omega\epsilon_0 Z^*, \tag{1}$$

$$\text{Conductivity: } \sigma^* = Z^{*-1}, \tag{2}$$

$$\text{Dielectric constant: } \epsilon^* = (\mathrm{i}\omega\epsilon_0)^{-1} Z^{*-1}, \tag{3}$$

where ε_0(= 8.85×10^{-12}F/m) is the permittivity of free space.

Ac conductivity measurements generate a large amount of data which can be represented and analyzed in a variety of ways. To aid the process, a number of procedures were developed for automated data handling and implemented as *Mathematica* notebooks and packages [2].

Table 1 The compositions of the silicon–polyester resin samples prepared

Sample name	Proposed silicon content (vol.%)	Measured silicon content (wt.%)	Calculated silicon content (vol.%)
PS0	0	0	0
PS4	4	8.3	4.1
PS5	5	9.3	4.7
PS8	8	17.6	9.3
PS12	12	22.3	12.1
PS16	16	28.9	16.3
PS20	20	35.3	20.7
PS24	24	41.7	25.5
PS28	28	47.1	29.9
PS32	32	51.8	34.0
PS36	36	53.7	35.7

Results and discussion

Composition and microstructure

Figure 1a and b shows optical micrographs of a silicon–polyester resin composite containing 16 vol.% silicon at two different magnifications. It can be seen, in both micrographs, that the particles of silicon are randomly dispersed in the polyester resin matrix and that at 16 vol.%, the silicon grains are quite far apart.

Figure 1c and d shows micrographs of a composite sample containing 36 vol.% silicon. Again the silicon is seen to be randomly dispersed within the polyester resin matrix. At 36 vol.%, the silicon particles, in two-dimensions, are now much more closely packed and, from the electrical measurements, there is a possibility of silicon–silicon contacts being formed in three-dimensions.

Figure 2 shows the regions immediately surrounding silicon grains, at higher magnification. It can be seen that the presence of the silicon particles causes some distortion of the polymer matrix. The disturbed regions around the silicon grains are almost certainly the silicon interfering with the curing of the polyester resin. This leads to the region around the grains setting at a different rate from the bulk of the polyester-resin matrix and the resulting stresses (strains) give rise to the disturbed region.

The frequency dependence of the electrical properties of silicon–polyester resin composites

The real dielectric constants and the real conductivities of various silicon–polyester resin composites (at all measured frequencies) are shown in Fig. 3. For clarity, the data from some of the samples investigated have been omitted from these plots. The omitted data show the same trends as are observed in the data presented. It will later be shown that all the samples studied are below the percolation threshold, φ_c.

No notable dispersion is observed in the dielectric constant of the pure polyester resin on the log scale, Fig. 3a, even at the lowest frequencies. For each of the samples containing silicon, the dielectric constant rises from a high frequency value (~8), through a shoulder at intermediate frequencies to a low frequency value greater than 10^3. It can also be seen that the dielectric constant at

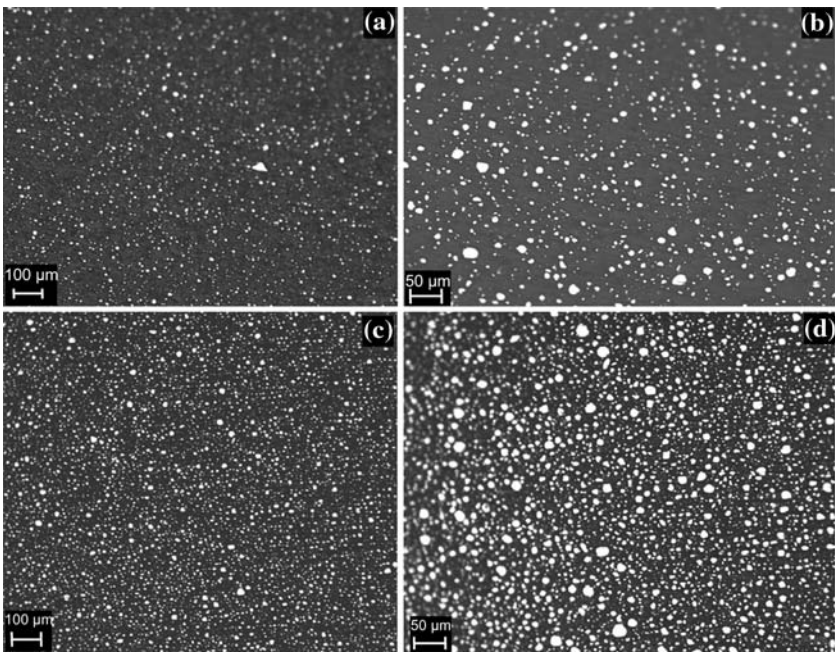

Fig. 1 Optical micrographs of a silicon–polyester resin composite containing 16 vol.% silicon, at low magnification (**a**) and higher magnification (**b**) and of the sample containing 36 vol.% silicon at, low magnification (**c**) and higher magnification (**d**)

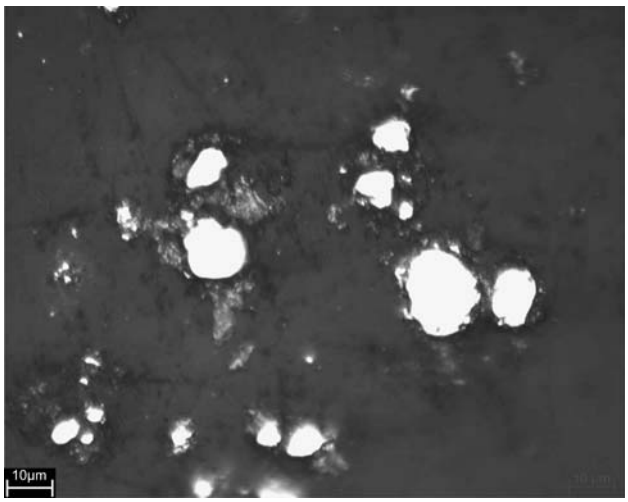

Fig. 2 High magnification optical micrograph of a silicon–polyester resin composite showing the region immediately surrounding the silicon grains

each frequency point increases as the volume fraction of the more conducting component (silicon) increases.

In Fig. 3b, going from the highest to the lowest frequencies, it can be seen that the conductivity of the pure polyester resin follows an unusual power law ($\sigma \propto \omega^n$), as the slope n is greater than 1, at high frequency, and then levels off to a flat region at intermediate frequencies. For the samples containing silicon, a partial shoulder, which becomes more pronounced with increasing silicon content, can just be seen at the highest frequencies ($\log(\omega) > 6$). Over a limited range of high frequencies the data follows a power law, dropping to a broader shoulder at intermediate frequencies. The data also shows a slow decrease at the lowest frequencies ($\log(\omega) < 0$).

Figure 4 shows the experimental real dielectric constant (on a log–linear scale) and the dielectric loss (on a log–log scale) for the pure polyester resin at $\log(\omega)$ above 0.5. The dielectric data is well modeled by the Havriliak–Negami (HN) expression [3], with two relaxation processes and a dc conductivity contribution:

$$\epsilon^*(\omega) = \epsilon' - \mathrm{i}\epsilon'' = -\mathrm{i}\left(\frac{\sigma_0}{\omega\epsilon_0}\right) + \sum_{k=1}^{2}\left[\frac{\Delta\epsilon_k}{\left(1 + (\mathrm{i}\omega\tau_k)^{\alpha_k}\right)^{\beta_k}} + \epsilon_{\infty k}\right], \quad (4)$$
$$0 \le \alpha, \beta \le 1,$$

where σ_0 is the dc conductivity, k is the number of relaxation processes, $\Delta\varepsilon_k$ is the difference in ε' at very low and at high frequencies for each relaxation process. The value of ε' at very high frequencies is ε_∞. τ_k is the relaxation time, α_k specifies the slope of the low frequency side of the relaxation in ε'' and β_k is the asymmetry parameter for each process [4].

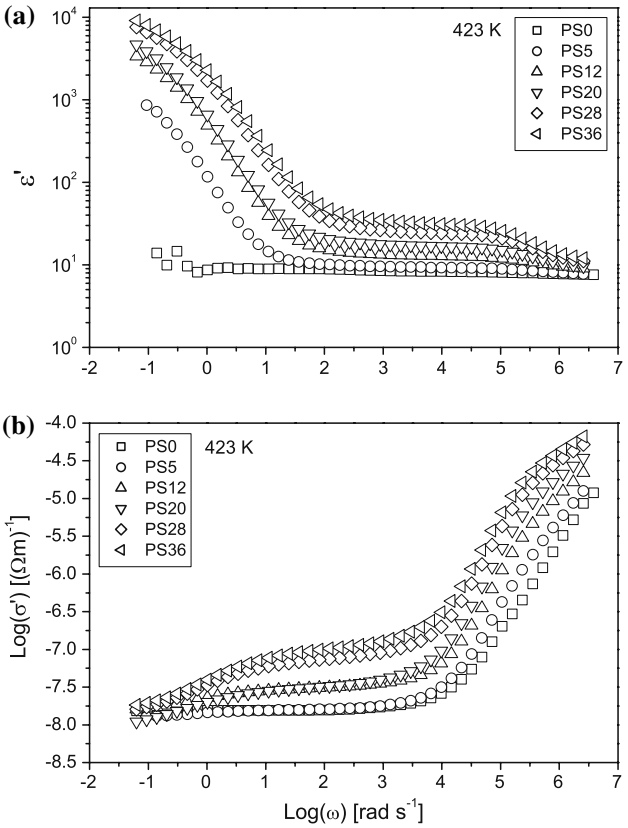

Fig. 3 The frequency dependence of the real dielectric constants and the real conductivities of some silicon–polyester resin composites at 150 °C

For the polyester resin at 150 °C, the best-fit parameters to the HN equation (Eq. 4), giving the line plotted in Fig. 4 are: $\sigma_0 = 1.55 \times 10^{-8}(\Omega\ \mathrm{m})^{-1}$, $\alpha_1 = 0.998$, $\alpha_2 = 0.499$, $\beta_1 = 0.418$, $\beta_2 = 0.292$, $\Delta\varepsilon_1 = 0.724$, $\Delta\varepsilon_2 = 3.10$, $\varepsilon_{\infty 1} = 4.97$, $\varepsilon_{\infty\ 2} = 0.177$, $\tau_1 = 0.00672$s and $\tau_2 = 6.91 \times 10^{-7}$s. The HN equation and the parameters, together with the TEPPE, will be used to simulate composite data over a wider frequency range than experimentally available.

The frequency dependence of the imaginary impedances and moduli of some of the silicon–polyester resin composites is shown in Fig. 5. For all frequencies above $\log(\omega) = 1$, the imaginary impedance, at each frequency point (Fig. 5a) decreases monotonically with increasing silicon content. This trend is to be expected, as the silicon is the more conducting component. It can also be seen that the characteristic frequency of the dominant peak in the composite data ($\log(\omega) \approx 2.3$), is essentially the same as that of the pure polyester resin (PS0) at this temperature. For the partial peak at lower frequencies ($\log(\omega) < 1$), there is a non-monotonic trend in $-Z''$, with increasing silicon content.

From Fig. 5b, it can be seen that the peak at low frequencies in the composite M'' data is associated with the

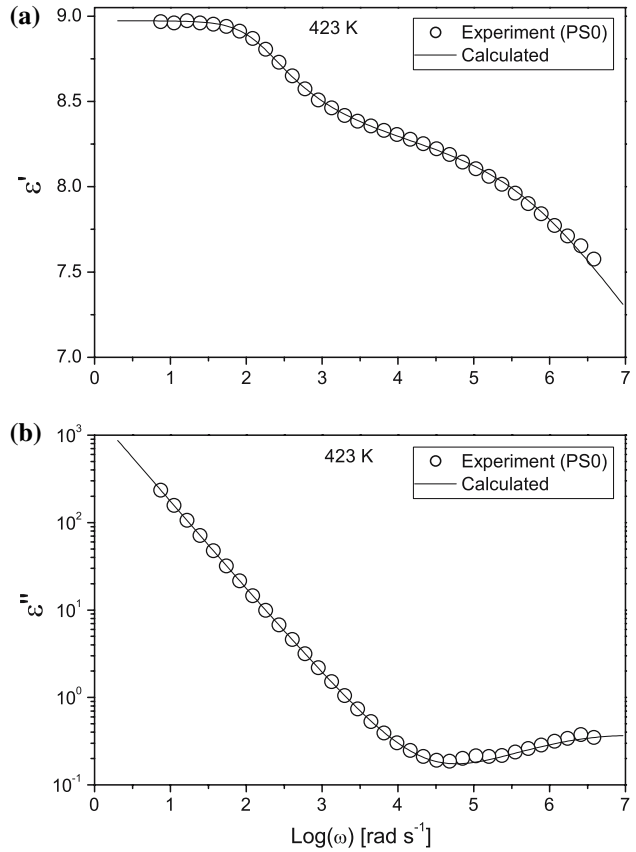

Fig. 4 The measured dielectric constant (**a**) and the dielectric loss (**b**) of the pure polyester resin at 150 °C fitted to Eq. 4. The parameters for the HN expression are given in the text

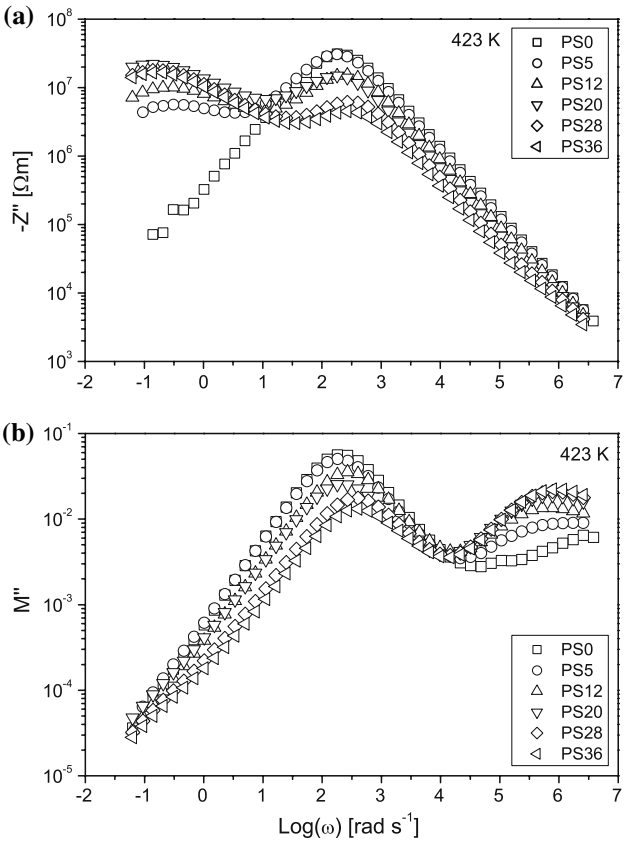

Fig. 5 The frequency dependence of the imaginary impedances (**a**) and imaginary moduli (**b**) of composites containing various volume fractions of silicon, at 150 °C

same dominant relaxation process as in the impedance spectra Fig. 5a. A partial peak is observed at high frequencies in the pure resin data. A much more pronounced high frequency peak is observed in the composite data. As this peak grows with silicon content it must therefore be associated with the silicon.

The central peak in the modulus and impedance data of the pure resin and the composites is clearly due to the primary relaxation process in the resin. The flat peaks at low frequencies in the imaginary impedance plot for the composites, which are not observed in the pure-resin (PS0) $-Z''$ plot and in all the imaginary modulus plots, are due either to interfacial and/or electrode polarization. In polymer composite systems, in addition to the high frequency process, two important aspects of induced polarization must be taken into account, at lower frequencies. The first is electrode polarization which results from the accumulation of ions at the polymer-electrode interface. The second aspect is the polarization due to the build-up of charges at the interface (or in the interphase) between the components. This polarization is known as the interfacial, space charge or Maxwell–Wagner–Sillars relaxation [5, 6]. Electrode and/or interfacial polarization (henceforth shortened to electrode/interfacial polarization) leads to an additional low frequency peak in the $-Z''$ plot but not in the M'' plot as they make a negligible contribution to the complex modulus (Moynihan et al. [7] and the references therein). From the results, the interfacial polarization is probably dominant, because the contribution of the interfacial/electrode effects to the impedance is increasing with the increasing silicon content (larger low frequency arc). Note that electrode/interfacial polarization has not been included in the fitting and simulations discussed later in this paper. The peaks seen at high frequencies in the dielectric modulus data indicate the presence of a component that is more conducting then the polyester resin.

Figure 6 shows the experimental complex *impedance* plane plots of the data for the samples PS0, PS5, PS20 and PS36. Only one arc, due to the polyester resin is observed for the pure polyester resin (Fig. 6a). Two arcs are observed in the complex impedance plane plots of the data for the composite samples PS5, PS20 and PS36 (Fig. 6b–d). One is due to the polyester resin matrix (high frequency) and the other due to electrode/interfacial polarization (low frequency).

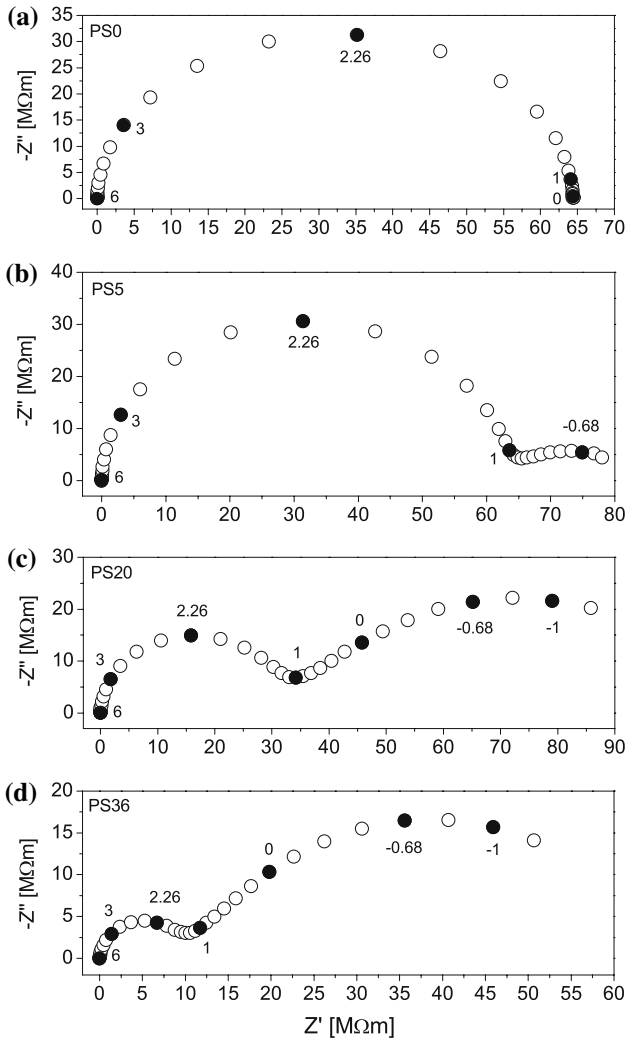

Fig. 6 Complex impedance plane plots of the data for the pure polyester resin and of composites containing various volume fractions of silicon. Key values of log(ω) are indicated in the plots

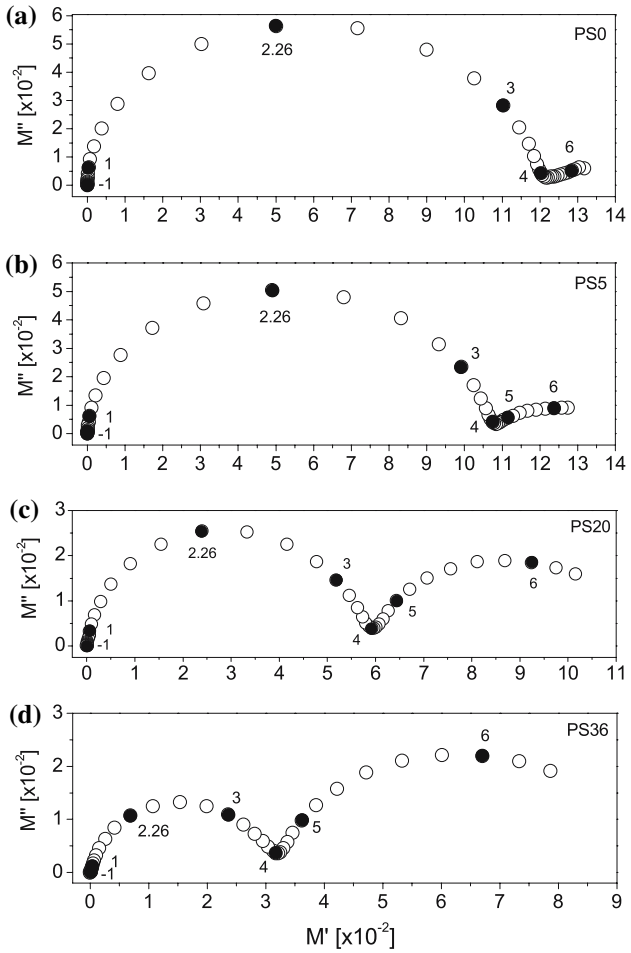

Fig. 7 Complex modulus plane plots of the data for the pure polyester resin and of composites containing various volume fractions of silicon. Key values of log(ω) are indicated in the plots

Figure 7 shows the complex modulus plane plots of the data for the samples PS0, PS5, PS20 and PS36. The modulus plot of the data for PS0 (Fig. 7a) shows one dominant arc and a small feature at high frequencies, which must be due to the secondary relaxation process in the polyester resin. A discussion on the mechanisms for the relaxation processes in polyester can be found in McCrum et al. [8]. For the composite sample PS5 (Fig. 7b), the complex modulus plane plot shows one complete arc and a partial arc at high frequency. This arc is more prominent than the feature at high frequencies in the data for PS0.

The complex modulus plane representations of the data for the samples PS20 and PS36 are shown in Fig. 7c and d. Two arcs are clearly observed in each of the data representations. Again the arcs in the complex modulus plane plots are attributed to the polyester resin (low frequency) and the silicon contribution (high frequency).

It will be shown below that the arcs at high frequencies in the modulus data of the composites, which are more prominent than the high frequency feature in the pure resin (PS0) data, are primarily due to the presence of a highly conducting component, the silicon. The presence of this conducting component leads to a high frequency feature in the data for the composites, which will later be shown to be percolation clusters, with a characteristic frequency similar to that of the secondary relaxation process in the pure resin.

The temperature dependence of the impedance and modulus of a silicon–polyester resin composite

The onset temperatures of the various processes contributing to the measured electrical properties of the polyester resin and the composites were investigated. Figure 8 shows the frequency dependence of $-Z''$ and M'' of the pure polyester resin at various temperatures. At all temperatures, only one peak is observed in the $-Z''$ (Fig. 8a). It can be

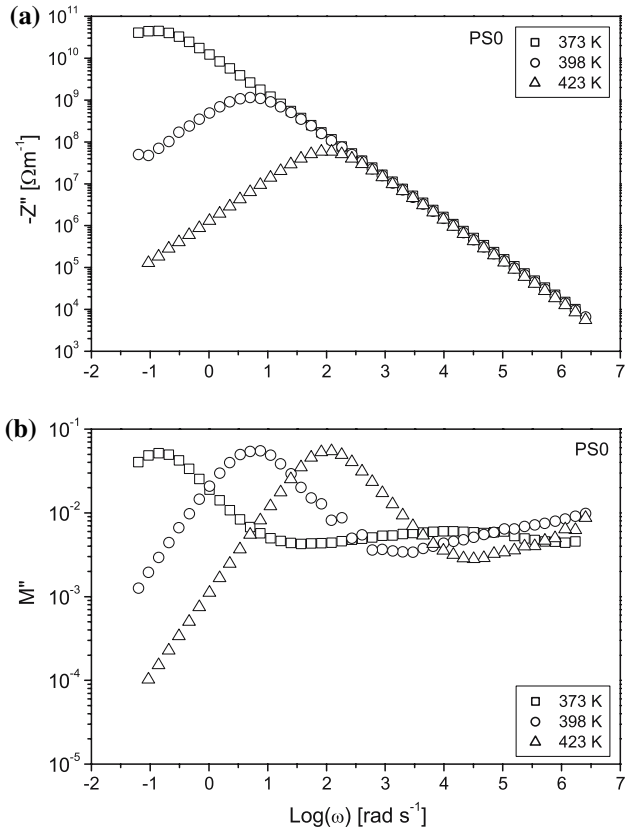

Fig. 8 The frequency dependence of the imaginary impedance and the imaginary modulus of the pure polyester resin at 100 °C, 125 °C and 150 °C

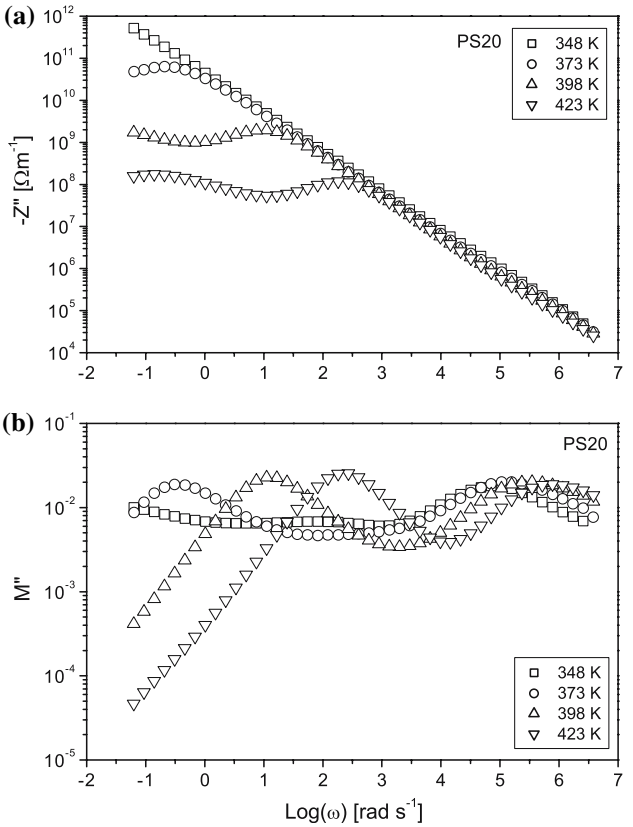

Fig. 9 The frequency dependence of the imaginary impedance and the imaginary modulus of the composite sample PS20 at 75, 100, 125 and 150 °C

seen in the M'' plot, Fig. 8b, that again there are two contributions to the modulus spectra. At 100 °C, the flat peak due to the high frequency relaxation process in the resin is well within the measured frequency range (max at $\log(\omega)\approx 4.5$) but above 125 °C the peak moves beyond $\log(\omega) = 7$.

Figure 9 shows the frequency dependence of $-Z''$ and M'' for the composite sample PS20 at various temperatures. At 75 °C, no peak is observed in the $-Z''$ plot, Fig. 8a. At 100 °C, one peak is observed at low frequencies while at 125 °C and at 150 °C, one complete and another partial low frequency peak are observed. The higher frequency peak is attributed to the polyester resin while and the other to electrode/interfacial polarization. The onset frequency at which electrode/interface polarization affects the experimental impedance is seen to increase with increasing temperature and sample conductivity. It can be seen in the M'' plot, Fig. 9b, that there are again two contributions to the modulus spectra. At all temperatures, except 75 °C, the peaks of both contributions are within the measurement range. This is unlike for the pure resin (Fig. 8b) where the peak of the high frequency contribution was beyond the range of the measurements for $T > 125$ °C. Again, the measurable high frequency contributions in the modulus spectra of the silicon rich composites must be attributed to the conductivity of the silicon.

Microstructure and the modeling of the electrical properties

Three models were considered for fitting the ac conductivity data of the composites. These are the Effective Media Maxwell–Wagner (MW) equation and Brick-Layer model (BLM), as well as the two exponent phenomenological percolation equation (TEPPE).

The Maxwell–Wagner equation is [9, 10]:

$$\frac{\sigma_m - \sigma_l}{\sigma_m + 2\sigma_l} - \phi\frac{\sigma_h - \sigma_l}{\sigma_h + 2\sigma_l} = 0, \tag{5}$$

where σ_h is the complex conductivity of the more conducting component and σ_l that of the less conducting (insulating) component. φ is the volume fraction of the more conducting component. This equation can also be written in terms of the complex permittivities (ε^*) or moduli (M^*). The Brick-Layer model equation [11] can be written as [2]:

$$\sigma_m = \frac{\sigma_l(\sigma_h + (\sigma_l - \sigma_h)\phi^{1/3} + (\sigma_h - \sigma_l)\phi)}{\sigma_h + (\sigma_l - \sigma_h)\phi^{1/3}}. \quad (6)$$

The microstructure described by the Maxwell–Wagner equation is discussed in detail in the review articles by McLachlan [9, 10] and that of the Brick-Layer model is described by Hwang et al. [11].

It was not possible to obtain satisfactory and consistent fitting results for the ac conductivity data of the silicon–polyester resin composites using either the Maxwell–Wagner equation or the Brick-Layer model, with the separately measured properties of the polyester resin and the actual volume fractions of silicon used in making the samples as input data.

Satisfactory and consistent results were obtained by fitting the data to the TEPPE, which has been applied successfully to a number of systems mostly for the analysis of dc conductivity results or single frequency ac data for varying conducting component volume fractions [12–16]. The TEPPE is:

$$(1-\phi)\frac{\sigma_l^{1/s} - \sigma_m^{1/s}}{\sigma_l^{1/s} + A\sigma_m^{1/s}} + \phi\frac{\sigma_h^{1/t} - \sigma_m^{1/t}}{\sigma_h^{1/t} + A\sigma_m^{1/t}} = 0, \quad (7)$$

where s and t are exponents and $A = \varphi_c/(1-\varphi_c)$. φ_c is the critical threshold for percolation. The TEPPE is applicable for finite values of the complex conductivities of both the more conducting and the insulating component. In order to determine both the percolation exponents, data must be available above and below the percolation threshold.

However, for the present system, where only samples with $\varphi < \varphi_c$ could be produced, the simplification, $s = t$, is used. This simplification is justifiable as the properties of a composite whose conductivity is described by Eq. 7 are dominated by the single exponent s [10] below φ_c.

Some of the results obtained from fitting the data are presented and discussed below. The following restrictions were imposed on the fitting:

- As mentioned above, the electrical properties of the polyester resin and the silicon volume fraction were fixed, at the separately measured values.
- The data from *all* the samples was fitted with common values for all the variable parameters. These are the exponent s, the percolation threshold φ_c and the complex conductivity of the more conducting component, the silicon.
- Since no straight forward model, or experimental results, could be found for the complex conductivity of the silicon powder at 150 °C, it was assumed that its properties were dispersionless and described by the expression $\sigma_h^*(\omega) = \sigma_h(0) + i\omega\varepsilon_0\varepsilon_h(0)$.

Figure 10 shows the dielectric constants and the conductivities of several silicon–polyester resin composites and the best fits to the experimental data obtained using the TEPPE with the separately measured electrical properties of the polyester resin and the measured silicon volume fractions as fixed input. φ_c, $\sigma_h(0)$, $\varepsilon_h(0)$ and $s(= t)$ were the variable parameters. The best-fitting parameter values, obtained from fitting the complex conductivity data from *all* the composite samples are $\sigma_h(0) = 3.50 \times 10^{-4}(\Omega\ \mathrm{m})^{-1}$, $\varepsilon_h(0) = 18$, $\varphi_c = 0.56$ and $s = t = 1.73$. With the exception of the sample with the highest silicon content (PS36), there is satisfactory agreement between the experimental and the calculated conductivities, at all but the lowest frequencies. There is also semi-quantitative agreement between the measured and the experimental dielectric constants.

Figures 11 and 12 show the complex impedance and modulus plane plots of the experimental data for the samples featured in Fig. 10 and the best-fitting results obtained using the TEPPE. While the fits to the impedance plots are satisfactory, with the possible exception of the sample with the highest silicon content (PS36), there is very good agreement between the model and the experimental data for the modulus plots. Even for sample PS36, there is qualitative agreement between the model and the data. The discrepancies between the measured and the calculated values at low frequencies could be due to too simple a model for the dispersive properties of the silicon and/or the onset of the low frequency interfacial or electrode effects.

Figure 13 shows the ''dc'' conductivities extracted from complex impedance plane plots (shown as circles), a simulation curve calculated using the TEPPE (continuous line) and simulation curves calculated using the Maxwell Wagner and the Brick-Layer models (dashed and dotted line respectively). The parameters for the TEPPE simulation, obtained from fitting the complex conductivity data, were ($\sigma_h(0) = 3.50 \times 10^{-4}(\Omega\ \mathrm{m})^{-1}$, $\varphi_c = 0.56$ (or 56%) and $s = t = 1.73$). Note the relatively high value of the percolation threshold (φ_c). Composites where the insulator coats the conducting component tend to have φ_c values above the value of 0.16 which is for equal sized spheres [10, 15, 17].

The extrapolated value $\sigma_l(0) = 1.54 \times 10^{-8}(\Omega\ \mathrm{m})^{-1}$ was used for the conductivity of the pure polyester resin. The experimental ''dc'' conductivities of the samples (extracted from the intercepts of the complex impedance plane plots with the real impedance axes) are in good agreement with the values calculated using the TEPPE, confirming the self consistency of the results of fitting the ac data. The simulations with the Maxwell–Wagner and Brick-Layer models were calculated using the same conductivity parameters as for the TEPPE simulation. It can clearly be seen that only the TEPPE simulation closely

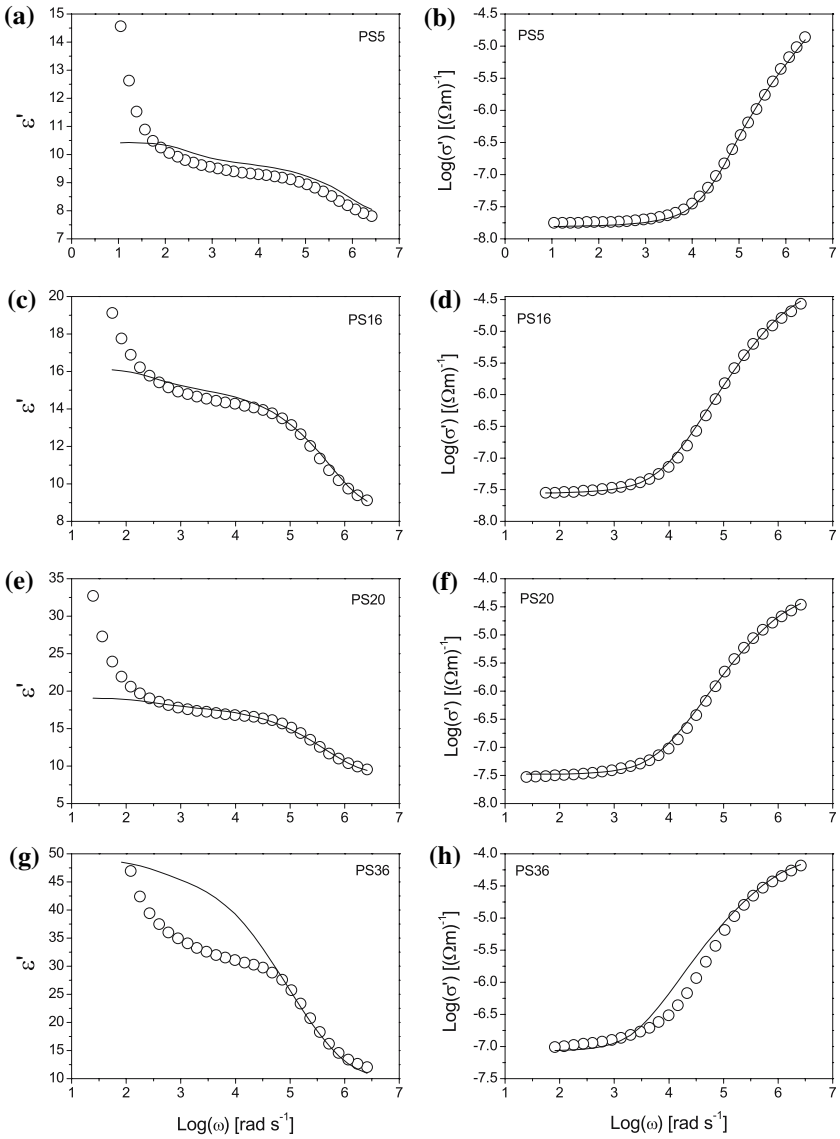

Fig. 10 The experimental values (circles) of the dielectric constant (**a**, **c**, **e**, **g**) and the conductivity (**b**, **d**, **f**, **h**) of four silicon–polyester resin composites and the results obtained from fitting the data to the TEPPE (*lines*) plotted as functions of log(ω)

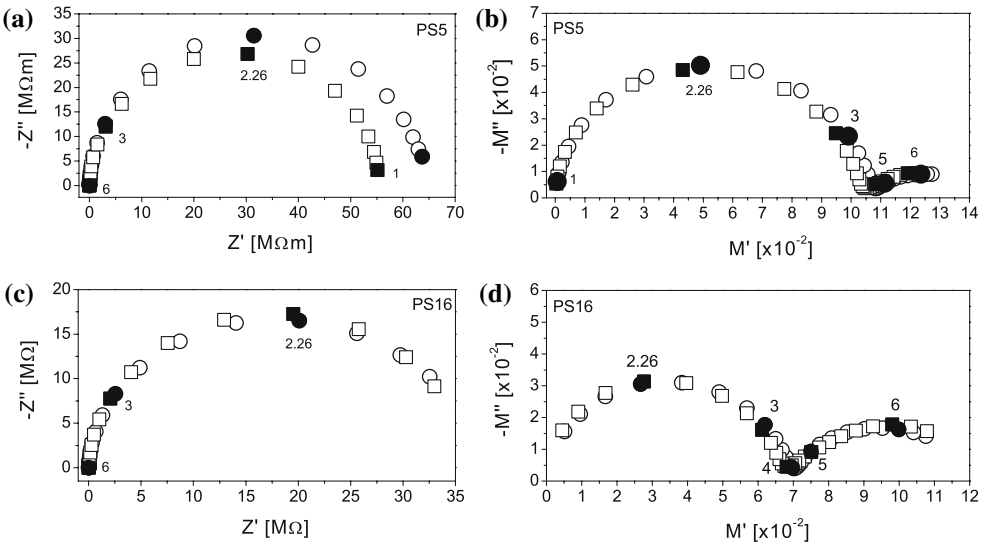

Fig. 11 Complex impedance and complex modulus plane plots of the experimental data (*circles*) and the best fit to the TEPPE (*squares*), for the samples PS5 and PS16. Key values of log(ω) are indicated in the plots

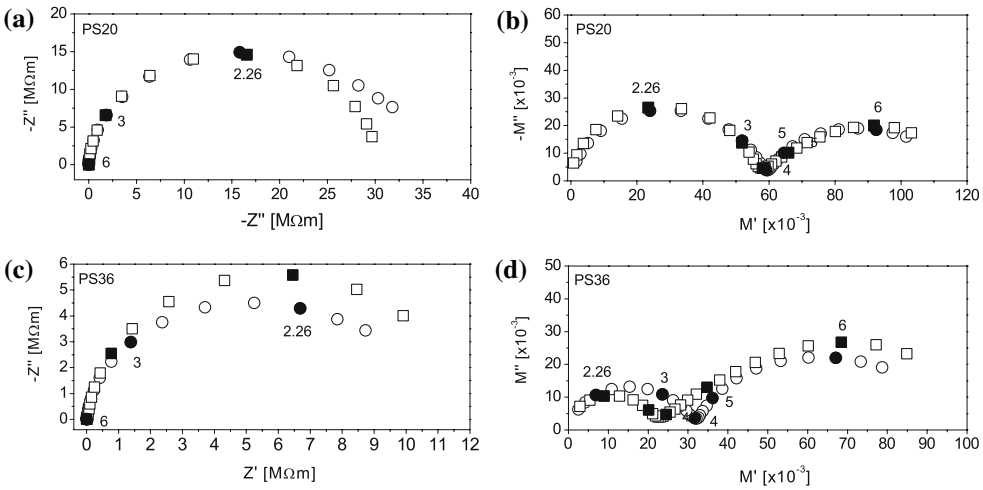

Fig. 12 Complex impedance and complex modulus plane plots of the experimental data (*circles*) and the best fit to the TEPPE (*squares*), for the samples PS20 and PS36. Key values of log(ω) are indicated in the plots

approximates the experimental data. Attempting to directly fit the ''dc'' data to the MW and BLM models, with variable $\sigma_h(0)$ and $\sigma_l(0)$, did not yield any fit better than those shown in Fig. 13. This confirms that the silicon–polyester resin system is a percolation system as it cannot be fitted to the effective medium (MW) or Brick-Layer model.

Figure 14 shows the dielectric loss measured for a number of composites containing tellurium (Te), silicon (Si) and germanium (Ge), made by the authors. It can clearly be seen that while the addition of each of the powders, with different conductivities, to the pure polyester resin causes an increase in the dielectric loss, a clear peak at high frequencies (arrow) is only observed for the samples containing silicon. This further supports the conclusion that the high frequency peak is due specifically to the conductivity of the silicon.

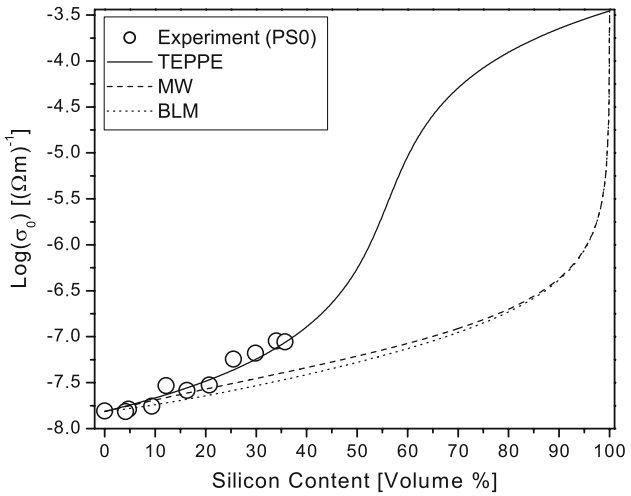

Fig. 13 The volume fraction dependence of the dc conductivity extracted from the complex impedance plane plots and simulations calculated using the TEPPE, BLM and MW equation. The parameter values used for the simulations are given in the text

The contributions to the measured properties of the silicon–polyester resin composites can be further understood by looking at the results of simulations calculated using the HN equation and the TEPPE. Figures 15 and 16 show the normalized imaginary impedances and moduli calculated using Eqs. 4 and 7 with $s = t$, for composites with a wider range of φ than could be explored experimentally. The use of the HN equation, with the parameters obtained from fitting the experimental polyester resin data, allows the simulation to be extended to frequencies beyond the range of the measurements. The conducting component properties are simulated using the best values which were obtained from fitting of the experimental composites' data as previously described. Note that in order to highlight particular features, while keeping the figures uncluttered, data for some φ values is shown in the modulus and not the impedance representation and vice versa. For lower φ the same values as obtained experimentally have been chosen for the simulations.

Figure 15 shows that the simulated sample imaginary impedance is dominated by the insulating component until φ_c. Well above φ_c, the impedance of the material is dominated by ''percolation clusters,'' whose characteristic frequencies ($-Z''$ peaks) are different from those of the pure insulating and conducting components [18]. Close to φ_c, the impedance of the percolation clusters is still somewhat dominated by the insulating component but by $\varphi = 0.8$, the impedance is dominated by the conducting component.

Figure 16 shows that even at very low φ values, the presence of the conducting component has a clearly observable effect on the modulus of the composite. For $0 < \varphi < \varphi_c$, two arcs, one associated with the pure insulator (and therefore having the same characteristic frequency, modulus peak) and the other with the ''percolation clusters,'' are observed. For $\varphi > \varphi_c$ a single peak is

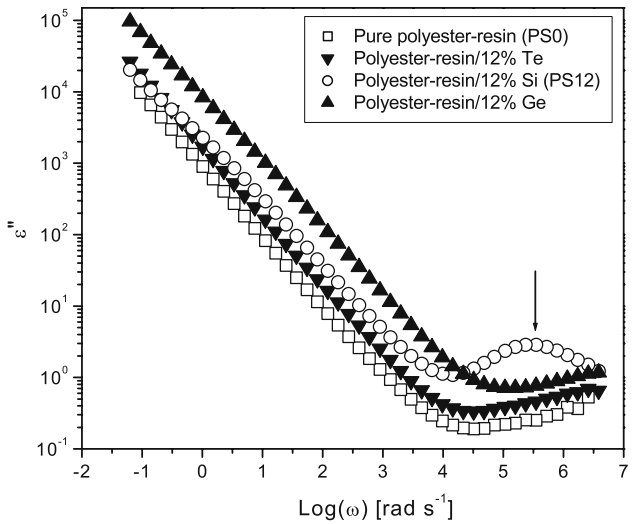

Fig. 14 The frequency dependence of the dielectric losses for various (polyester resin + 12%*x*) composites at 150 °C

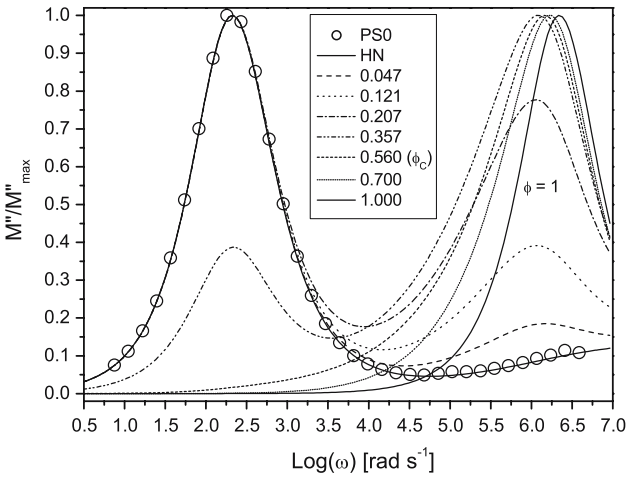

Fig. 16 The frequency dependence of the normalized imaginary modulus data, for the pure polyester resin (PS0) and for composite simulations, with a wide range of conducting component volume fractions (φ), calculated using the HN equation and the TEPPE. Note that the $\varphi = 0$ or pure HN simulation is labeled ''HN''

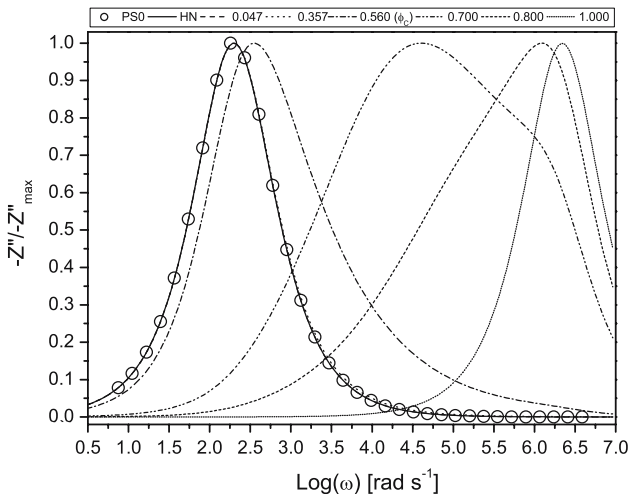

Fig. 15 The frequency dependence of the normalized imaginary impedance data, for the pure polyester resin (PS0) and for composite simulations, with a wide range of conducting component volume fractions (φ), calculated using the HN equation and the TEPPE. Note that the $\varphi = 0$ or pure HN simulation is labeled ''HN''. Note that the $\varphi < \varphi_c$ curves (i.e. $\varphi = 0.047$ and $\varphi = 0.357$) are hidden under the *solid curve* obtained using the HN equation over the entire frequency range

observed. Note that the modulus peaks associated with the ''percolation clusters,'' lie at slightly lower frequencies than the conducting component peak. For composites where the ratio of the conductivities of the components is higher than that in the current simulations by an order of magnitude or more, the percolation clusters and the components have clearly distinct characteristic frequencies and can therefore readily distinguished [18].

Conclusions

In the current paper, the electrical properties of silicon–polyester resin composites have been discussed. In addition to the dominant effects of the polyester resin matrix, two distinct contributions are observed in the modulus and impedance data of the composites. These are attributed to electrode/interfacial effects (low frequency $-Z''$) and percolation effects (high frequency primarily in M''). These contributions can only be resolved and clearly identified by using both the impedance and modulus representations of the data. The paper clearly illustrates the importance of using various representations of the immittance spectroscopy data in order to correctly identify the contributions of the components to the measured properties of composites. As it is a percolation system, it can only be satisfactorily fitted to the two exponent phenomenological percolation equation (TEPPE). This model fits the data consistently, using the experimentally measured properties of the polyester resin as well as volume fractions of the silicon as fixed input.

Acknowledgements GS would like to acknowledge financial assistance from the TW Khambule GOOT Fellowship at the University of the Witwatersrand.

References

1. Novocontrol GmbH, Hundsangen, Germany (1994) Novocontrol broadband dielectric converter BDC: Owner's manual
2. Sauti G (2005) Electrical conductivity and permittivity of ceramics and other composites. PhD thesis, Physics, University of the Witwatersrand, Johannesburg

3. Havriliak S, Negami J (1966) J Polym Sci C 14:99
4. Schaumburg G (1995) Dielectrics Newslett, 9–12
5. Mijovic J, Fitz BD (1998) Novocontrol Applic Note Dielectrics 2
6. Perrier G, Bergeret A (1997) J Polym Sci Part B Polym Phys 35(9):1349
7. Howell FS, Bose RA, Macedo PB, Moynihan CT (1974) J Phys Chem 78(6):639
8. McCrum NG, Read BE, Williams G (1967) Anelastic and dielectric effects in polymeric solids. Wiley, New York
9. McLachlan DS, Hwang JH, Mason T (2000) J Electroceram 5(1):37
10. McLachlan DS (2000) J Electroceram 5(2):93
11. Hwang JH, McLachlan DS, Mason T (1999) J Electroceram 3(1):7
12. Wu J, McLachlan DS (1997) Phys Rev B56(3):1236
13. Xia J, Pan Y, Shen L, Yi XS (2000) J Mater Sci 35:6145
14. Youngs IJ (2000) IEE Proc Sci Meas Tech 147(4):202
15. Youngs IJ (2001) Electrical percolation and the design of functional electromagnetic materials. Ph.D. thesis, Electronic and Electrical Engineering, University College, London
16. McLachlan DS, Chiteme C, Park C, Wise KE, Ounaies Z, Lowther SE, Lillehei P, Siochi EJ, Harrison JS (2005) J Polym Sci Part B Polym Phys 43:3273
17. Kusy RP (1977) J Appl Phys 48(12):5301
18. Chiteme C, McLachlan DS, Sauti G (2007) Phys Rev B 75:094202